Synthesis and characterisation of Fe and [Fe,Al]-MCM-22 zeolites

Testa, F.; Crea, F.; Diodati, G.D.; Pasqua, L.; Aiello, R.; Terwagne, Guy; Lentz, Patrick; B.Nagy, Janos

Published in:
Microporous and Mesoporous Materials

DOI:
10.1016/S1387-1811(99)00029-3

Publication date:
1999

Document Version
Early version, also known as pre-print

ELSEVIER

Microporous and Mesoporous Materials 30 (1999) 187–197

MICROPOROUS AND MESOPOROUS MATERIALS

Synthesis and characterization of Fe- and [Fe,Al]-MCM-22 zeolites

F. Testa [a,*], F. Crea [a], G.D. Diodati [a], L. Pasqua [a], R. Aiello [a], G. Terwagne [b], P. Lentz [c], J.B. Nagy [c]

[a] *Department of Chemical and Materials Engineering, University of Calabria, 87030 Rende (CS), Italy*
[b] *L.A.R.N., Facultés Universitaires Notre-Dame de la Paix, 5000 Namur, Belgium*
[c] *Laboratoire de R.M.N., Facultés Universitaires Notre-Dame de la Paix, 5000 Namur, Belgium*

Abstract

The synthesis of Fe-MCM-22 zeolite is reported for the first time. Its structure and characteristics are similar to those of the MCM-22 zeolite. The aluminum is in a framework tetrahedral position in the [Fe,Al]-MCM-22 samples. The white color of the samples, the increase of the ^{29}Si and ^{27}Al NMR linewidths with increasing Fe content and the constancy of the (Fe + Al)/u.c. values all suggest that Fe is also incorporated in tetrahedral position of the framework.

Keywords: Characterization; MCM-22; Iron; Synthesis; Zeolite

1. Introduction

MCM-22 is synthesized under hydrothermal conditions using an organic template (generally hexamethyleneimine) and inorganic cations [1,2]. The hexagonal structure contains two different independent porous systems. The first consists of a two-dimensional sinusoidal channel system, accessible through 10-ring apertures. The layers containing this channel system are linked together by oxygen bridges forming large supercages characterized by 12-ring apertures of 7.1 Å inner free diameter and an inner height of 18.2 Å [3,4].

In recent years the properties of MCM-22 have been thoroughly investigated [5–7]. Dealuminated acid forms of MCM-22 have been characterized, concluding that the acidic properties are very similar to a H-ZSM-5 zeolite [6]. Synthesis parameters for the preparation of MCM-22 zeolite have been optimized. Only a low Si/Al ratio is convenient for the synthesis of pure MCM-22 [7].

^{27}Al and ^{29}Si MAS NMR studies on as-synthesized and dealuminated samples revealed that the framework silicon and aluminum atoms are located on at least five crystallographically non-equivalent tetrahedral (T) sites [6]. Certain ^{29}Si NMR lines were characterized by T sites that are distant from template molecules [8].

Catalytic properties, cracking of alkanes, isomerization of *m*-xylene, hydroisomerization of *n*-decane, etc. were also studied but they are only mentioned in this context.

In this paper we report for the first time the synthesis and characterization of Fe-MCM-22 zeolite. While this paper was being examined by the referees a short communication appeared in the literature [9].

* Corresponding author. Fax: +39-984-493-073.
E-mail address: f.testa@unical.it (F. Testa)

1387-1811/99/$ – see front matter
PII: S1387-1811(99)00029-3

2. Experimental

Two different methods of synthesis are necessary in order to obtain [Fe,Al]-MCM-22 and pure [Fe]-MCM-22, respectively. For example, pure [Fe,Al]-MCM-22 was obtained by mixing 0.31 g of $Al(OH)_3$ (Pfaltz and Bauer), 6.4 g of NaOH (Carlo Erba, 30% weight solution in water) and 7.2 g of fumed SiO_2 (Serva) in 64.8 g of distilled water, so obtaining a solution named A. At the same time, 2.58 g of $Fe(NO_3)_3 \cdot 9H_2O$ (Merck) was dissolved in 32.4 g of distilled water, forming the solution named B. After complete homogenization solution B was added drop by drop to solution A. Finally, the synthesis mixture was obtained by adding 5.95 g of hexamethyleneimine (HMI, Aldrich). The experimental protocol is similar to that used for the preparation of ferrisilicate ZSM-5 zeolites [9–12]. For the procedure of synthesis reported here, white [Fe,Al]-MCM-22 (samples 2, 3, 4, see Table 1) products were obtained and brown [Fe]-MCM-22 (sample 5). The general composition of the gels was: $6Na_2O$–$30SiO_2$–aAl_2O_3–$bFe(NO_3)_3$–15HMI–$1350H_2O$ with $a=0$, 0.2, 0.5 and 0.8 and $b=2$, 1.6, 1 and 0.4, respectively. (Note that $Al+Fe=2$ in the gel.)

A white crystalline sample of [Fe]-MCM-22 (sample 1, Table 1) was synthesized using the following procedure: 2.58 g of $Fe(NO_3)_3 \cdot 9H_2O$ and 7.2 g of fumed SiO_2 were added to 64.8 g of distilled water in order to obtain an iron silicate gel. Simultaneously, 6.4 g of NaOH (30% weight solution in water) was added to 32.4 g of distilled water. This solution was added drop by drop to the iron silicate gel and, after complete homogenization, 5.95 g of hexamethylenimine (Aldrich) was mixed, obtaining the final synthesis mixture: $a=0$ and $b=1.6$ in the gel.

Syntheses were carried out in PTFE autoclaves under dynamic conditions (33 rounds per minute) at a temperature of 150°C. The crystallinity of the samples was determined by comparing the intensity of the peaks in X-ray diffraction spectra with the reference spectrum of an MCM-22 sample previously synthesized and taken as standard. X-ray diffraction spectra ($d=3.42$ or 26.1° 2θ) for the as-synthesized and calcined samples were collected on a Philips PW1710 diffractometer. A Cu Kα lamp was powered with 40 kV and 20 mA. Data were acquired in the 2θ range 5–40° with a step size of 0.02° and a step time of 5 s.

Samples 2, 3 and 4 exhibit 100% crystallinity after 7 days of synthesis of the reaction mixture. Samples 1 and 5 show complete crystallization only after 11 days. In Table 1 the reaction mixture ratios are reported.

Samples were calcined in dry air flow of 10 cm^3/min at a temperature of 600°C for 6 h. The heating rate was 1°C/min.

Measurements of nitrogen adsorption at 77 K were carried out using a Micromeritics ASAP 2010 apparatus. About 80 mg of the calcined sample was degassed at 473 K and $\sim 10^{-6}$ mmHg before the acquisition of data.

Thermal analysis (DSC and TG) was carried out using a Netzsch Model STA 409. The samples were run from room temperature to 800°C at a rate of 10°C/min under 15 cm^3/min flow of dry air.

Atomic absorption analyses were carried out with a Shimadzu AA-660 spectrometer. About 200 mg of the calcined samples was dissolved with

Table 1
Composition of the initial gel leading to Fe-MCM-22 and [Fe,Al]-MCM-22 at 150°C

Sample	Si/Al+Fe	Fe/Al	OH/tet.[a]	Na/tet.	HMI/tet.	H_2O/tet.	Color
1	20	8	0.38	0.38	0.48	42.9	White
2	15	4	0.375	0.375	0.47	42.2	White
3	15	1	0.375	0.375	0.47	42.2	White
4	15	0.25	0.375	0.375	0.47	42.2	White
5	15	8	0.375	0.375	0.47	42.2	Brown

[a] tet = moles Si + moles Al + moles Fe.

5 ml of HF and 2 ml of H_2SO_4 and diluted in distilled water at the desired volume.

EPR spectra were reported at room temperature on a Bruker BER-420 spectrometer with a TE102 rectangular cavity.

The NMR spectra were recorded either on a Bruker MSL400 or on a CXP200 spectrometer. For ^{29}Si (39.7 MHz), a 6 μs ($\theta=\pi/2$) pulse was used with a repetition time of 6.0 s. For ^{27}Al (104.3 MHz), a 1.0 μs ($\theta=\pi/12$) pulse was used with a repetition time of 0.1 s. For ^{13}C (50.3 MHz), a 15 μs ($\theta=\pi/2$) pulse was used with proton high power decoupling.

For IR studies, thin self-supporting wafers of each sample were prepared and outgassed under vacuum, in a home-made cell, at temperatures of 550°C for 3 h. The IR spectra were taken on a FT-IR Bruker IFS-28 with a resolution of 2 cm^{-1}.

The ion exchange experiments were carried out as follows: 0.5 g of the calcined product was treated three times with a 1 M NH_4NO_3 aqueous solution (10 ml solution/g of solid) at 80°C. After each ion exchange the solid was filtered and washed with distilled water. The NH_4 form was calcined in air at 550°C for 6 h. The so-obtained H form of the products was ion exchanged with a 1 M KCl solution following the same procedure as the first exchange. The K form of the microporous solid was dried for 12 h at 120°C.

Transmission Mössbauer spectroscopy was also used to determine the site occupied by iron. The technique provides information about the local environment of the ^{57}Fe nuclei randomly distributed throughout the sample by measuring the perturbation of nuclear levels resulting from the interaction with local, internal magnetic fields and with the external electric field. The Mössbauer measurements were made using a ^{57}Co source in a Rh matrix with an activity of 50 mCi. The specimen of interest was placed between the source and a Si(Li) detector where 14.4 keV γ rays resulting from the recoilless resonant absorption of ^{57}Fe nuclei within the specimen were detected.

3. Results and discussion

The X-ray powder diffractogram shows clearly that the as-synthesized solid has the structure of MCM-22 zeolite [Fig. 1(a)]. Tables 2 and 3 show the comparison between the line positions and their relative intensities for the sample MCM-22 and the literature data [1]. Before calcination most of the lines are broad and overlap. The calcined Fe-MCM-22 sample also shows the characteristics of calcined MCM-22 [5] [Fig. 1(b) and Tables 2 and 3).

SEM photographs of the as-synthesized Fe-MCM-22 samples 2, 3 and 5 are shown in Fig. 2. They are very similar to those reported for the MCM-22 zeolite samples [7,13]. The thin platelets of ca. 1–2 μm diameter frequently form spherical aggregates of ca. 10–15 μm and the morphology does not depend on the Fe content. Calcination of the samples did not affect the morphology of the crystals.

In Table 4 are reported the content of iron, aluminum and sodium determined by atomic absorption and the content of the organic molecule trapped in the zeolite channels determined by thermogravimetric analysis. The values are expressed in moles per 100 g of activated samples,

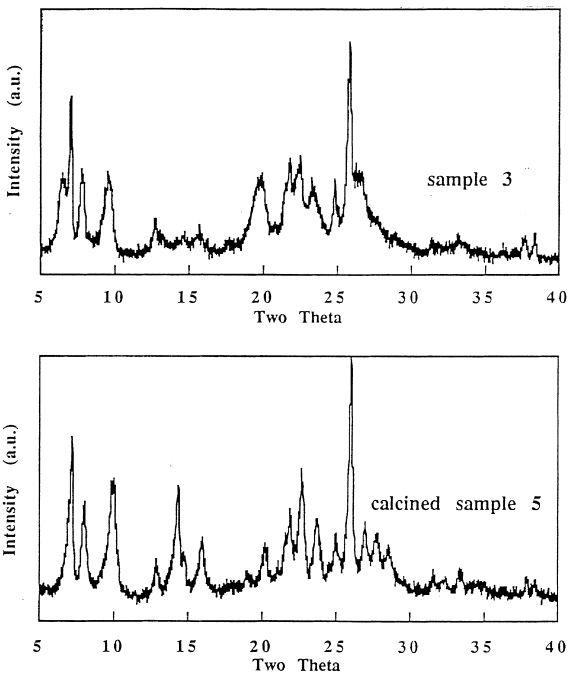

Fig. 1. XRD patterns of the as-made [Fe,Al]-MCM-22 sample 3 and of the calcined Fe-MCM-22 sample 5.

Table 2
Comparison between X-ray powder diffraction patterns of as-made sample 3 and precursor MCM-22

As-made		MCM-22[a]	
$d(hkl)$	I_{rel}	$d(hkl)$	I_{rel}
13.63	57.6	13.53	36
12.51	70.9	12.38	100
11.30	51.9	11.13	34
9.17	48.4	9.14	20
6.94	34.7	6.89	6
6.76	29.7	6.68	4
6.08	28.3	6.02	5
4.44	53.5	4.47	22
4.08	57.4	4.05	19
3.95	58.8	3.95	21
3.79	48.0	3.77	13
3.58	48.2	3.57	20
3.44	100	3.43	55
3.39	53.8	3.36	23
3.07	31.2	3.06	4
2.69	29.8	2.68	5
2.38	29.7	2.38	5
2.34	27.3	–	–

[a] From Ref. [5].

Table 3
Comparison between X-ray powder diffraction patterns of calcined sample 5 and calcined MCM-22

Calcined		MCM-22 calcined[a]	
$d(hkl)$	I_{rel}	$d(hkl)$	I_{rel}
12.34	71.0	12.34	100
11.07	50.3	11.02	51
8.85	58.5	8.90	46
6.16	55.8	6.17	35
5.54	37.7	5.55	13
4.38	36.5	4.38	10
4.10	39.9	4.11	10
4.05	47.6	4.06	20
3.91	61.3	3.82	29
3.75	45.9	3.75	15
3.56	40.4	3.56	14
3.42	100	3.42	61
3.30	43.6	3.30	13
3.21	40.5	3.21	9
3.06	28.2	3.12	6
2.68	28.4	2.68	6
2.37	26.4	2.37	4
2.34	25.2	–	–

[a] From Ref. [5].

i.e. the sample from which the water and the organic molecules were removed. The sum of iron and aluminum incorporated in the MCM-22 structure is quite constant and the Fe/Al ratio is always greater than in the reaction mixture (4.6, 1.3 and 0.5 for samples 2, 3 and 4, respectively). The sodium content is very low compared to the trivalent atoms content.

The amount of HMI is equal to 0.20 mol% and is not dependent on the trivalent atoms in the structure. As the amount of (Fe + Al) is equal to ca. 0.09 mol% and the Na amount is much smaller than this value (it varies from 0.003 to 0.009 mol%) (Table 4), some 0.081 mol% of protonated HMI has to neutralize the framework negative charges linked to both Al and Fe (see below).

The DSC curves show clearly that there are two peaks for the HMI decomposition, one with a maximum of ca. 380°C and the other at ca. 465–500°C (Fig. 3). The temperature of the low temperature peak only very slightly depends on the Al/u.c. (Table 4), while the position of the high temperature peak increases with increasing framework Al content. (In fact, a linear relation is obtained for the variation of T_{max} as a function of Al content.) This means, that these HMI molecules and/or ions interact more strongly with the framework negative charges linked to the presence of Al.

The ratio of the amount of HMI decomposed at high temperature to that decomposed at low temperature varies from 1/0.65 to 1/1.2. The low temperature HMI species were shown to occupy the interlayer supercages in MCM-22 zeolite, while the high temperature HMI species are occupying the intralayer zig-zag channels [5]. The HMI/u.c. values vary from 9.2 to 9.6. The occupation of the supercages is characterized by 3.9–5.8 HMI/u.c., while the intralayer occupancy varies from 4.3 to 5.8. (These values were computed from a formula weight of one unit cell equal to 4825 given in Ref. [5].) As the (Fe + Al)/u.c. values are close to 4.3 and the Na/u.c. values are only equal to 0.14 (or 0.44), almost half of the HMI species have to be in the protonated form neutralizing the framework negative charges.

The two different HMI species cannot be shown by the ^{13}C NMR spectrum, because it is not well resolved due to the presence of the paramagnetic

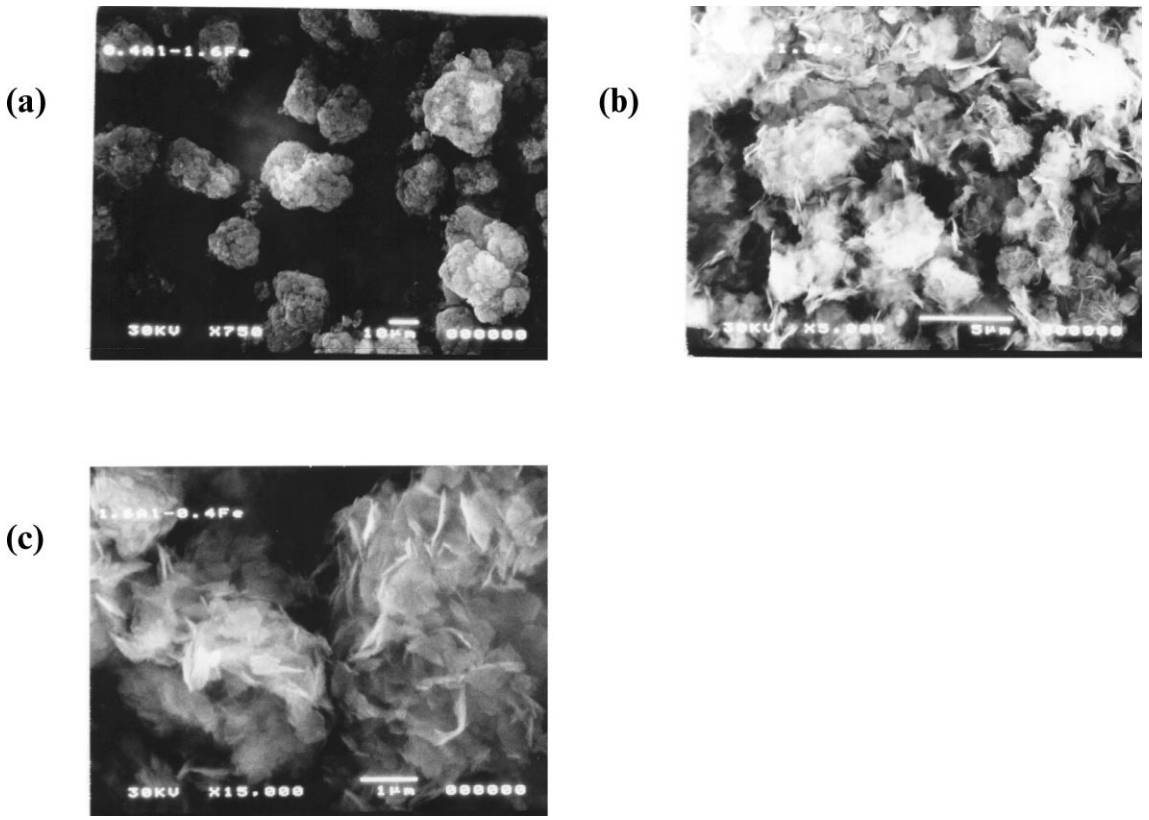

Fig. 2. Scanning electron micrographs of [Fe,Al]-MCM-22 samples 2 (a) and 3 (b) and of Fe-MCM-22 sample 5 (c).

Fe(III) in the framework (Fig. 4). Note that only the ^{13}C NMR spectrum of the low Fe-containing sample 4 could be measured.

The Al atoms are well introduced into the structure in a tetrahedral form. Indeed, the chemical shift of ca. 54 ppm characterizes tetrahedral species of $Al(OSi)_4$ configuration (Fig. 5 and Table 5). It is not possible to detect different Al species in the structure, as was the case for MCM-22 zeolite [5,6], because of the line broadening due to the Fe(III) species, although some asymmetry can be recognized in the spectrum

Table 4
Chemical analysis of the as-made [Fe,Al]-MCM-22 and Fe-MCM-22 samples[a,b] and ion exchange capacities of the corresponding calcined samples

Sample	Fe[a] ($\times 10^{-2}$ mol%)	Al[a] ($\times 10^{-2}$ mol%)	Si/ Al+Fe	Na[a] ($\times 10^{-2}$ mol%)	K/ (Al+Fe)	Fe_{tetr} (%)	HMI[b] ($\times 10^{-2}$ mol%)	DSC peaks (°C)–HMI[b] ($\times 10^{-2}$ mol%)	
1	7.8	–	19.9	0.28	0.40	40	19	377.6–8	466.3–11
2	7.4	1.6	17.1	0.56	0.48	36	20	384.1–10	479.4–10
3	5.3	4.1	16.4	0.91	0.71	49	20	385.7–9	490.8–11
4	3.5	6.3	15.8	0.30	0.83	80	20	384.4–11	502.8–9
5	9.3	–	16.5	0.69	0	0	20	376.7–8	464.6–12

[a] Atomic absorption.
[b] Thermal gravimetry.

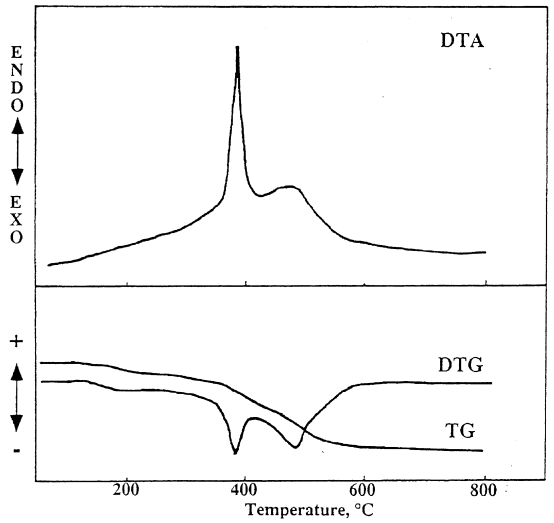

Fig. 3. DSC, TG and DTG curves of Fe-MCM-22 sample 2.

(Fig. 5). The ^{27}Al NMR linewidth increases with increasing Fe(III) content in the samples (Fig. 6).

The linewidths do not differ very much for the calcined samples (Fig. 5 and Table 5). However, for the higher Fe content samples 2 and 3 a new broad NMR line appears at ca. 30 ppm which could be either due to extraframework Al species very much broadened due to extraframework Fe species or to deformed Al species in the structure. Work is in progress to identify the various Al species in the Fe-MCM-22 samples.

While the Fe/u.c. increases from 1.7 to 4.5, that of Al/u.c. decreases from 3.0 to 0.8 and their sum remains constant for the different samples. This means that the Fe species and the Al species are in competition and the introduction of a total of 4.3 = (Fe + Al)/u.c. is favored in our reaction conditions.

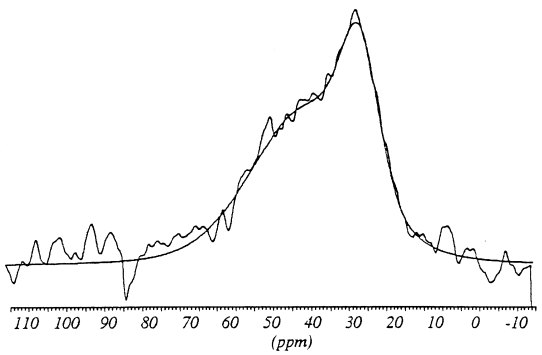

Fig. 4. ^{13}C NMR spectrum of Fe-MCM-22 sample 4.

The ^{29}Si NMR spectra of the samples are centered at ca. −110 ppm (Fig. 7 and Table 6). They do not show any fine structure due to the presence of paramagnetic Fe(III) species, which lead to line broadening. The NMR linewidth increases linearly with increasing Fe content of the samples (Fig. 5). The increase is much smaller for the calcined samples suggesting that part of the Fe(III) ions have left the zeolite framework.

The color of the as-made samples is white except for sample 5, where some brownish color was detected, showing the presence of extraframework Fe-containing species.

EPR results were used to characterize the Fe species in the zeolite samples. One typical spectrum of sample 3 is recorded in Fig. 8 and Table 7 shows the g values of the various Fe-containing species. Despite the great importance of the EPR technique in characterizing the various paramagnetic species, no clear-cut interpretation has been given until now. For example, the species characterized by a g factor of 2.0 are considered octahedral [14,15], while such species are described as framework tetrahedral species in Ref. [16]. The signal at $g = 2.3$ is considered as the $g_{\parallel}$ contribution of the octahedral species [14,15]. Finally, at $g = 4.3$ can be found the framework tetrahedral species, the intensity of which is higher at low temperatures [14]. This species can be included in the EPR signal observed at low magnetic field, where only the middle of the spectrum was computed to be between 4.23 and 4.56. The latter species are considered as deformed tetrahedral species.

The Mössbauer spectra of the Fe-MCM-22 as-made samples confirm the presence of tetrahedral Fe(III) ions (Table 8 and Fig. 9). The spectra of samples 1 [Fig. 9(a)] and 5 [Fig. 9(b)] were decomposed by attempting to use two doublets, one for the tetrahedral configuration of Fe, and one for the octahedral configuration. The resulting parameters are listed in Table 8. The isomer shift of tetrahedrally coordinated Fe(III) is equal to 0.18 mm/s for both samples. Octahedrally coordinated Fe(III) is detected in sample 5 and is characterized by higher isomer shift (0.32 mm/s) and quadrupolar splitting (0.93 mm/s). These

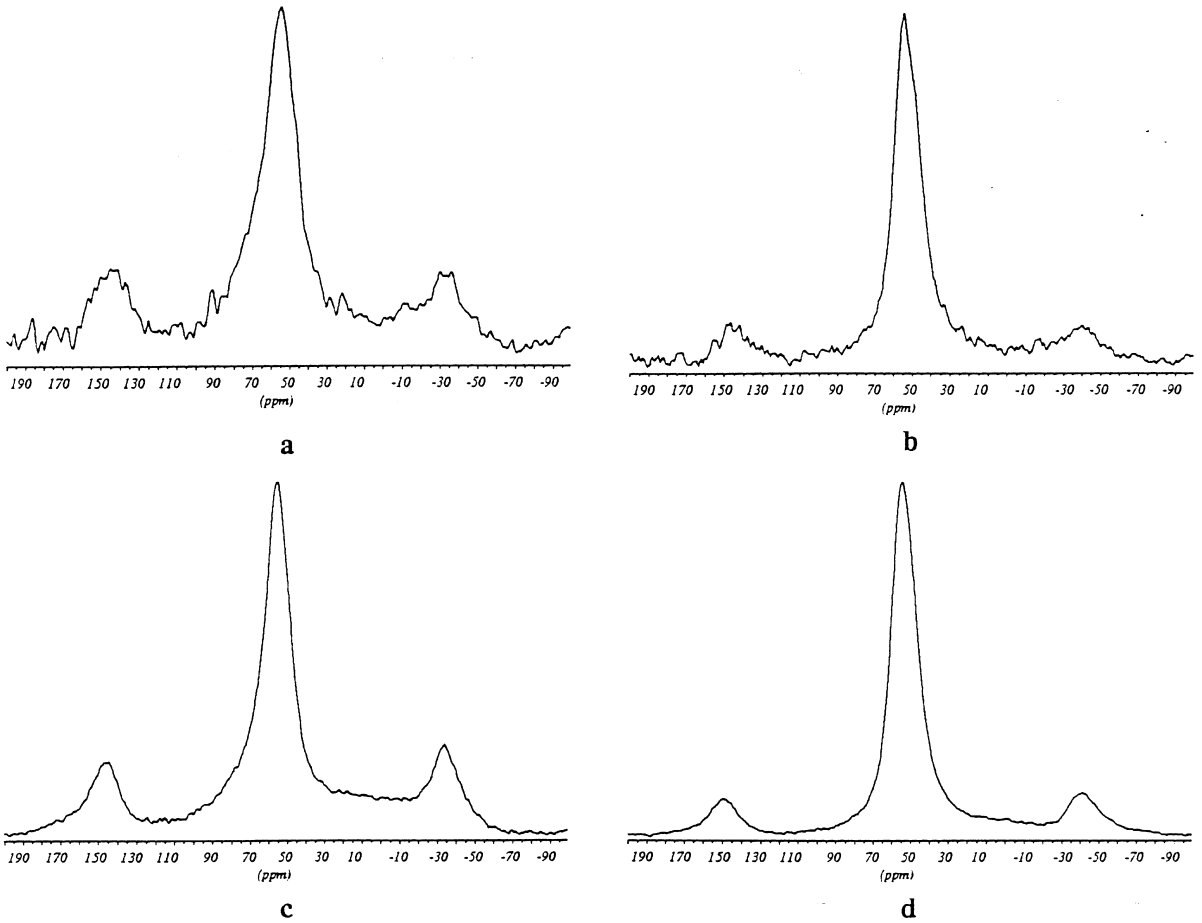

Fig. 5. ^{27}Al NMR spectrum of Fe-MCM-22 samples 3 and 4. Sample 3 as-made (a); sample 4 as-made (b); sample 3 calcined (c); sample 4 calcined (d).

Table 5
^{27}Al NMR data of precursor Fe-MCM-22 samples (a) and calcined Fe-MCM-22 samples (b)

	(a)		(b)	
Sample	δ (ppm)	ΔH (Hz)	δ (ppm)	ΔH (Hz)
1	–	–	–	–
2	54	2930	55.6 (~30)	2800 (7000)
3	53.4	2000	55.6 (~30)	1600 (7000)
4	55.0	1520	55.0	1550
5	–	–	–	–

values are in good agreement with those reported in the first genuine publication by Meagher et al. [17] and later confirmed by others [18–20]. It is

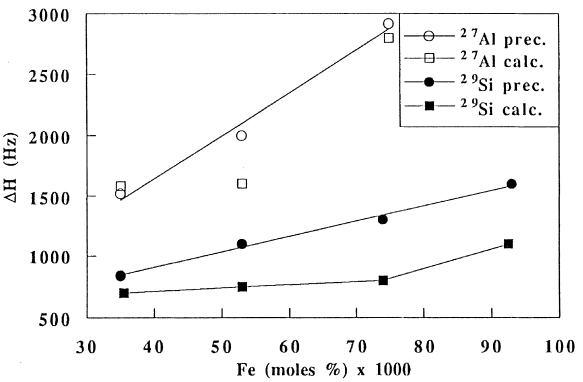

Fig. 6. Variation of the ^{27}Al and ^{29}Si NMR linewidths as a function of Fe content of the [Fe,Al]-MCM-22 samples.

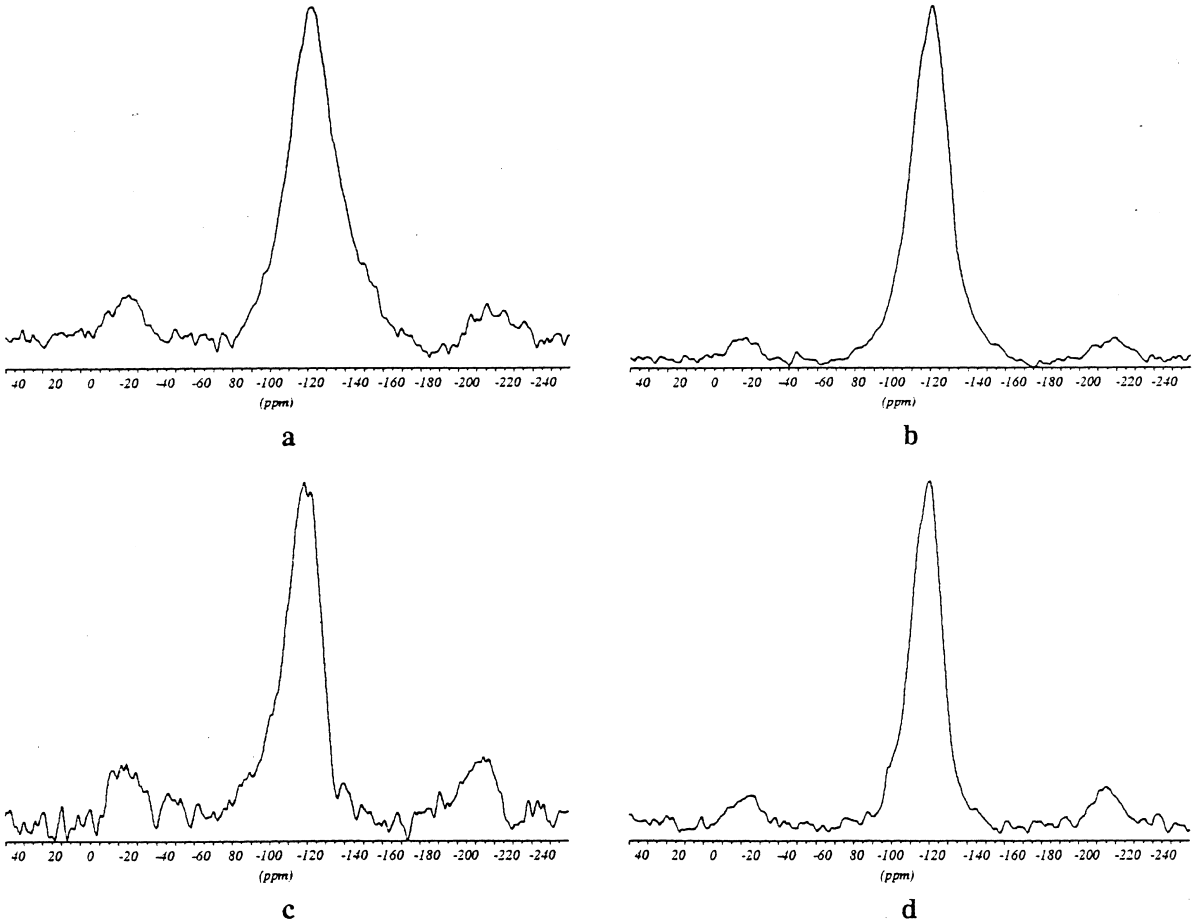

Fig. 7. ^{29}Si NMR spectra of [Fe,Al]-MCM-22 samples 3 and 4. Sample 3 as-made (a); sample 4 as-made (b); sample 3 calcined (c); sample 4 calcined (d).

Table 6
^{29}Si NMR data of precursor Fe-MCM-22 samples (a) and calcined Fe-MCM-22 samples (b)

	(a)		(b)	
Sample	δ (ppm)	ΔH (Hz)	δ (ppm)	ΔH (Hz)
1	−113	400 (1000)	−113	400 (1000)
2	−106	1300	−109	800
3	−108	1100	−110	750
4	−110	850	−109	700
5	−108	1500	−110	1100

interesting to note that despite the brownish color of sample 5, the amount of tetrahedral Fe(III) is still high (some 87%).

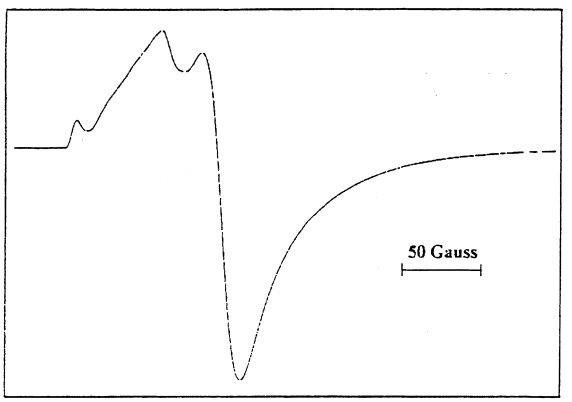

Fig. 8. Room temperature EPR spectrum of as-made [Fe,Al]-MCM-22 sample 3.

Table 7
EPR results of as-made Fe-MCM-22 zeolite samples taken at room temperature

Sample	g		
1	4.263	2.307	1.985
2	4.559	2.440	2.017
3	4.497	2.449	2.011
4	4.381	2.437	2.012
5	4.446	2.451	2.169

Table 8
Mössbauer isomer shift (IS), quadrupole splitting (QS) and relative intensities (I_{rel}) of Fe-MCM-22 as-made samples taken at room temperature[a,b]

Sample		IS (mm/s)	QS (mm/s)	I_{rel} (%)
1	$Fe(III)_{tetra}$	0.18	0.40	100
	$Fe(III)_{octa}$	–	–	–
5	$Fe(III)_{tetra}$	0.18	0.38	87
	$Fe(III)_{octa}$	0.32	0.93	13

[a] The spectra were measured at ± 10 mm/s velocity.
[b] The average error is ca. ± 0.03 mm/s.

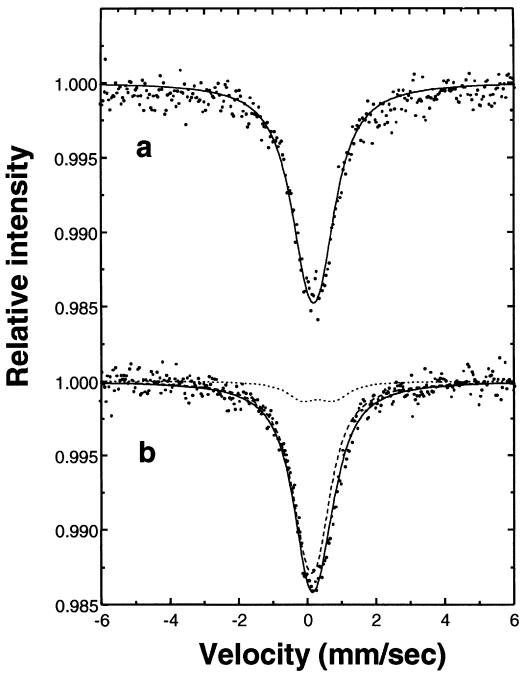

Fig. 9. Room temperature Mössbauer spectra of the calcined Fe-MCM-22 samples 1 and 5.

FT-IR and ion exchange measurements were carried out on the calcined samples. Indeed, both techniques are very important to assess the framework or extraframework position of the M(III) elements.

The introduction of M(III) elements into the tetrahedral framework of zeolites generates Si(OH)M Brönsted acid sites. This is clearly shown in Fig. 10, where the 3800–3400 cm^{-1} region is expanded. The position of the maximum of the 3620 cm^{-1} band shifts to higher wavenumbers when the Al content of the sample decreases. The values of the maxima are 3622 cm^{-1} for sample 4, 3627 cm^{-1} for sample 3, 3639 cm^{-1} for sample 2 and 3640 cm^{-1}. The band at ca. 3730 cm^{-1} stems from internal SiOH groups. The presence of the 3640 cm^{-1} band in sample 1 strongly suggests that Fe(III) occupies a tetrahedral framework position in this Fe-MCM-22 material [9]. Fe-MCM-22 sample 5 also contained tetrahedral framework Fe(III) (see for example the above Mössbauer spectra), the calcined sample does not show clearly the presence of Fe(III) in the framework. The higher wavenumber observed for Si(OH)Fe with respect to Si(OH)Al groups [9] also suggests that the Brönsted acidity of Fe-MCM-22 is much weaker than that of Al-MCM-22.

The ion exchange capacities are very interesting.

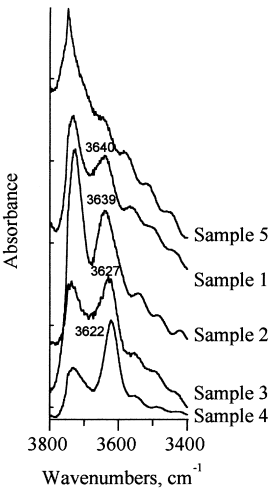

Fig. 10. FT-IR spectra of the calcined Fe-MCM-22 (1 and 5) and [Fe,Al]-MCM-22 samples.

The K/(Al+Fe) ratios are reported in Table 4. The ion exchange capacity is clearly linked to framework M(III) elements [10,21]. The K exchange capacity increases from the Fe-MCM-22 sample (number 1) to the highest Al content [Fe,Al]-MCM-22 (sample 4). It is also interesting to compute the relative percentage capacity with respect to the Fe(III) content of the as-made samples. These values are also reported in Table 4. They were computed from the K/(Al+Fe) values supposing that the state of aluminum did not change during calcination. This was not verified for samples 2 and 3 (see the ^{27}Al NMR results of Table 5) and the so-computed values are somewhat underestimated. It can be seen that some 40% of Fe(III) remain in framework position after calcination of Fe-MCM-22 zeolite. The presence of Al seems to contribute to the stability of Fe(III) in the structure. Indeed, the percentage tetrahedral Fe(III) is as high as 80% in the presence of the highest Al content (sample 4).

Specific surfaces and microporous volumes were measured by BET techniques and the Horvàth–Kavazoe plot. These values together with the average pore dimensions are reported in Table 9. The S_{BET} surfaces are smaller, while the micropore volumes are larger than those reported previously [13,22].

4. Conclusions

In conclusion, the constancy of the (Fe+Al)/u.c. values in the as-made samples, the white color of the as-made samples, the Mössbauer spectra, the dependence of both the ^{27}Al and ^{29}Si NMR linewidths on the Fe content of the samples all show that a great part of the Fe is in a tetrahedral framework position in the Fe-MCM-22 zeolites. The Brönsted acidity and the ion exchange capacity show that a non-negligible part of Fe(III) remains in tetrahedral framework position even after air calcination of the samples. The synthesis of Fe-containing MCM-22 could open new routes for catalysis involving oxido-reduction reactions.

Table 9
Sorption characteristics of Fe-MCM-22 zeolite

Sample	S_{BET} (m^2/g)	V (cm^3/g)	d (Å)
1	308	0.221	12.64
2	302	0.217	12.65
3	308	0.236	12.65
4	317	0.229	12.90
5	334	0.241	12.91

Acknowledgements

The authors are indebted to Mr. Guy Daelen for his skilful help in taking the NMR spectra. The present work is a part of a project coordinated by A. Zecchina and cofinanced by the Italian MURST (Cofin 98, Area 03). The work was also supported by Regione Calabria (POP 1994/99). P. Lentz gratefully acknowledges financial support from F.R.I.A., Belgium.

References

[1] M.K. Rubin, P. Chu, US Patent 4,954,325, 1990.
[2] C.D. Chang, D.M. Mitke, US Patent 5,173,281, 1992.
[3] M.E. Leonowicz, J.A. Lawton, S.L. Lawton, M.K. Rubin, Science 264 (1994) 1910.
[4] G.J. Kennedy, S.L. Lawton, M.K. Rubin, J. Am. Chem. Soc. 116 (1994) 11000.
[5] S.L. Lawton, A.S. Fung, G.J. Kennedy, L.B. Alemany, C.D. Chang et al., J. Phys. Chem. 100 (1996) 3788 and references cited therein.
[6] M. Hunger, S. Ernst, J. Weitkamp, Zeolites 15 (1995) 188.
[7] A. Corma, C. Corell, J. Pérez-Pariente, Zeolites 15 (1995) 2.
[8] R. Ravishankar, T. Sen, S. Sivasanker, S. Ganapathy, J. Chem. Soc., Faraday Trans. 91 (1995) 3549.
[9] P. Wu, H. Lin, T. Komatsu, T. Yashima, Chem. Commun. (1997) 663.
[10] R. Szostak, T.L. Thomas, J. Catal. 100 (1986) 555.
[11] R. Szostak, T.L. Thomas, J. Chem. Soc., Chem. Commun. (1986) 113.
[12] R. Szostak, Molecular Sieves: Principles of Synthesis and Identification, Van Nostrand Reinhold, New York, 1989.
[13] R. Ravishankar, R. Bhattacharyer, N.E. Jacob, S. Sivasankar, Micropor. Mater. 4 (1995) 83.
[14] B. Wichterlova, L. Kubelkova, P. Jiru, D. Kolihova, Collect. Czech. Chem. Commun. 45 (1980) 2143.
[15] J. Varga, J. Halasz, D. Horvàth, D. Méhn, J.B. Nagy, G.

Schabel, I. Kiricsi, Proc. Capoc4, 9–11 April, Brussels, Belgium (1997) , in press.
[16] G. Catana, J. Pelgrims, R.A. Schoonheydt, Zeolites 15 (1995) 475.
[17] A. Meagher, V. Nair, R. Szostak, Zeolites 8 (1988) 3.
[18] K. Lázár, G. Borbély, H. Beyer, Zeolites 11 (1991) 214.
[19] A. Hagen, F. Roessner, I. Weingart, B. Spliethoff, Zeolites 15 (1995) 270.
[20] P. Fejes, J.B. Nagy, K. Lázár, J. Halász, Appl. Catal., submitted.
[21] R. Szostak, V. Nair, T.L. Thomas, J. Chem. Soc., Faraday Trans. I 83 (1987) 487.
[22] A. Corma, C. Covell, J. Pérez-Pariente, J.M. Guil, R. Guil-Lopez, S. Nicolopulos, J. Gonzalez Calbert, M. Vallet-Regi, Zeolites 16 (1996) 7.